Response to comments by reviewers 2#:

We really appreciate you for your carefulness and conscientiousness. We will benefit impressively from your suggestions about writing and technique details.

After carefully reading the revised opinions, we have made all the changes suggested by the reviewer and addressed all the comments in the notes below. All the changed contents are highlighted in blue in the revised manuscript.

Overall comments：

Perturbations to PSD parameters:

1) **No explanation of how the assumed perturbations in parameters were determined, or what sources were used to justify the assumptions. E. g., Line 284 "According to the range in b, the standard deviation (SD) as assumed to be 0.5 and 0.3 for snow and graupel".**

Response: Thanks very much for the valuable comment. The relevant information has been added, and the SD of *b* has been recalculated.

"According to results from observation experiments reported in the literatures, the exponent *b* for snow varies from 1.4 to 2.8, and most of the mass relations have the mean value of *b* close to 2.1(Brandes et al., 2007; Heymsfield et al., 2010; Huang et al., 2019; Sy et al., 2020; Szyrmer and Zawadzki, 2010; Tiira et al., 2016; Wood et al., 2013). For graupel, the exponent *b* varies from 2.1 to 3 (Heymsfield et al., 2018; Mason et al., 2018; Von Lerber et al., 2017), with a mean value of approximately 2.6. Based on the range and mean value of *b* for the Gaussian distribution, we calculated the standard deviation (SD) to be 0.28 and 0.16 for snow and graupel, respectively."

2) **Overall, the explanations of the sensitivity analysis falls short, particularly as related to PSD perturbations. For example, when "a" is increased, does the reflectivity increase because of the resulting change in the scattering properties of individual particles, or is it because the ice water content increased? When "a" was increased, was N_w decreased so that the ice water content was unchanged? The same sort of concern applies to the evaluation of sensitivities for other PSD parameters.**

Response: Thanks very much for your valuable suggestion. when "a" is increased, the reflectivity increases mainly due to the change in the scattering properties. The PSD was slightly changed to keep the water content unchanged. The part of the sensitivity analysis for PSD perturbations have been rewritten.

"An exponential PSD with a power-law mass spectrum was used for snow and graupel. Figure 4 shows the effects of intercept parameter N_0 and the mass power-law parameters of prefactor *a* and exponent *b*. With the mean mass-size relationships for snow and graupel, changing the dBN_0 ($dBN_0 = \log_{10}(N_0)$) from 3 to 5 could cause a reflectivity increase of approximately 7–8 dB, as shown in Fig. 4a and d. The mass power-law parameters vary with snow/graupel type, shape, and porosity. In

Fig. 4b and e, we see that with a constant N_0 and mean value of exponent *b*, the reflectivity change caused by variation in prefactor *a* from 0.005 to 0.013 g/cm^b for snow and 0.02 to 0.06 g/cm^b for graupel (*W* remains constant) can reach 7–10 dB. An increase in *a* lead to an increase in the corresponding particle scattering properties. The intercept parameter N_0 will slightly decrease with the increase in *a* implicitly representing the effects of aggregation at warmer temperatures (Woods et al., 2008). Among them, the change to particle scattering properties caused by the perturbation of *a* play a dominant role in the reflectivity change. Using an average mass-power relation assumption, the variation in *a* as a result of the degree of aggregation and riming, and particle shapes may result in the reflectivity uncertainty of approximately 45 % and 30 % for snow and graupel, respectively. For analyzing the effect of the variation in *b*, a Gaussian distribution of *b* was modeled. According to results from observation experiments reported in the literatures, the exponent *b* for snow varies from 1.4 to 2.8, and most of the mass relations have the mean value of *b* close to 2.1(Brandes et al., 2007; Heymsfield et al., 2010; Huang et al., 2019; Sy et al., 2020; Szyrmer and Zawadzki, 2010; Tiira et al., 2016; Wood et al., 2013). For graupel, the exponent *b* varies from 2.1 to 3 (Heymsfield et al., 2018; Mason et al., 2018; Von Lerber et al., 2017), with a mean value of approximately 2.6. Based on the range and mean value of *b* for the Gaussian distribution, we calculated the standard deviation (SD) to be 0.28 and 0.16 for snow and graupel, respectively. The error bars in Fig. 4c and f represent the SD of the reflectivity change caused by variation in *b*, which was approximately 2 dB for snow and 0.5 dB for graupel. The results showed that the sensitivity of reflectivity to prefactor *a* was substantially greater than that of exponent *b*. In all, the mass relationships that depend on particle habits and formation mechanisms, cause substantial uncertainties in W-band radar reflectivity. Our results are consistent with the sensitivity analysis by Wood and L'Ecuyer (2021) who pointed out that the W-band radar reflectivity uncertainty for snowfall was dominated by the particle model parameter (e.g., the prefactors and exponents of the mass relationships). The mass relationship can cause the reflectivity uncertainty of several to more than 10 dB. The results indicate that improved constraints on assumed particle mass models would improve forward-modeled radar reflectivity and physical parameter retrieval."

3) I suggest also looking at Wood and L'Ecuyer, 2021, AMT. How do your sensitivity results compare to their conclusions about sources of uncertainty in retrieved snowfall?

Response: Thank very much for the valuable suggestion. We have carefully read the literature (Wood and L'Ecuyer, 2021), and compared our results with those in Wood and L'Ecuyer (2021). Wood and L'Ecuyer (2021) showed that the contributions to uncertainties in W-band radar reflectivity from the particle model parameters (e.g., the coefficients and exponents of the mass relationships) was most substantial, which may cause 5 to 15 dB reflectivity uncertainty. Our study shows that he reflectivity change caused by variation in prefactor *a* from 0.005 to 0.013 g/cm^b for snow and 0.02 to 0.06 g/cm^b for graupel (*W* remains constant) can reach 7–10 dB. The reflectivity change caused by variation in *b* was approximately 0.5-2 dB. The mass relationships cause substantial uncertainties in W-band radar reflectivity. Our results are consistent with those in Wood and L'Ecuyer (2021). The comparison with Wood and L'Ecuyer (2021) has been added in the revised manuscript.

"Our results are consistent with the sensitivity analysis by Wood and L'Ecuyer (2021) who pointed out that the W-band radar reflectivity uncertainty for snowfall was dominated by the particle model parameter (e.g., the prefactors and exponents of the mass relationships). This relationship can cause the reflectivity uncertainty of several to more than 10 dB. The results indicate that improved constraints on assumed particle mass models would improve forward-modeled radar reflectivity and physical parameter retrieval."

WRF model simulations:

1) **Details of how the model simulations were performed are lacking. Sufficient details should be provided to reproduce the simulations. In particular, information about the microphysical parameterizations should be provided, but also other details such as nested domain sizes, positions, time steps, vertical gridding should be included. This information could be provided in an appendix.**

Response: Thank you very much for the valuable suggestion. Details of WRF model simulations have been added in the Appendix A.

"Appendix A: Model setup and verification

a. Stratiform case

The simulation for this stratiform case was conducted with four nested grids (d01, d02, d03, and d04), and the inner domain was centered at 41.08°N, 117.61°E. The horizontal grid spacings are 27km, 9km, 3km, and 1km and the corresponding grids are 120×120, 180×180, 300×300, and 300×300. The vertical resolution increases with height from approximately 50 m near the surface to 600 m near 50 hPa. Time steps of 180s and 6.67s were used for d01 domain and d04 domain, respectively. The 6-hourly NCEP FNL operational global analysis data on 1° × 1° grids were used to provide the initial and boundary conditions. In term of physical scheme, the model adopted CAM 5.1 5-class scheme, Grell-Freitas cumulus parameterization scheme, RRTM long and short-wave radiation scheme, YSU boundary layer scheme, Monin-Obukhov surface layer scheme and thermal diffusion land surface scheme. The cumulus parameterization scheme was used for d01 and d02 domains only.

Besides the cloud fraction and cloud top temperature shown in Fig. 8, the cloud water path (CWP) from MODIS was used for model result verification as well. Figure A1a is the cloud water path calculated from vertical integration of WRF output cloud water over d01 domain at 03:30 UTC, 25 September, and Fig. A1b is the cloud water path from MODIS Level 2 product at 03:35 UTC, 25 September 2012. The scanning width of MODIS is 2330 km, and the horizontal resolution for the product of CWP is 1 km. The CWP distribution of model result has similar pattern as MODIS observation and the value of CWP are close, but the peaks of the two are slightly offset. Due to the measurement techniques and model limitations, the model simulations may be biased from the observations. However, the distribution, structure, and value of CWP from model and MODIS observation generally agree well.

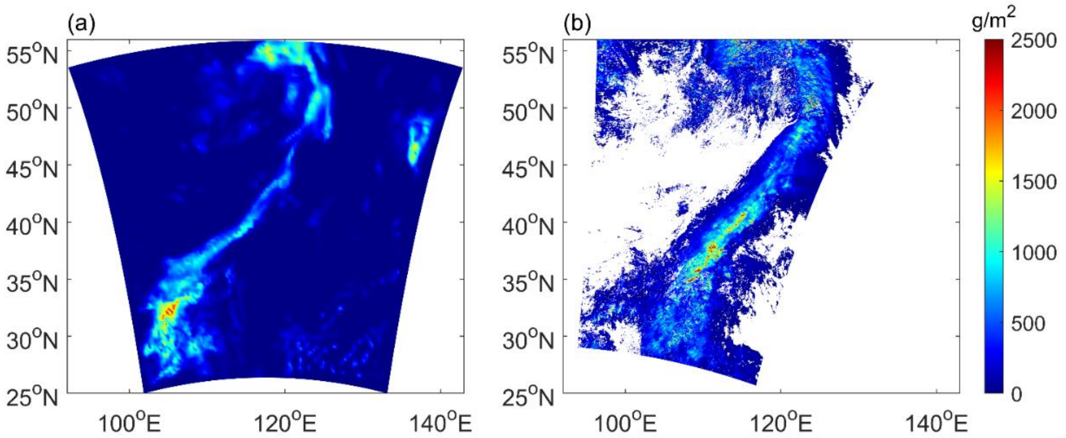

Figure A1: Comparison of CWP between the WRF model result and MODIS data for the stratiform case. (a) CWP from the WRF model at 03:30 UTC, (b) CWP from MODIS observation at 03:35 UTC, 25 September 2012.

b. Convective case

For the convective case, three nested grids (d01, d02 and d03) with horizontal grid spacings of 22.5km, 7.5km, and 1.5km and corresponding grid points of 70×70, 126×126, and 280×280 were used for the convective case simulation. The inner domain d03 is centered at 34.02°N, 118.20°E. A total of 39 vertical layers with stretch spacing from the surface to 50 hPa were used, with time steps of 90, 30, and 6 s for d01, d02 and d03, respectively. The initial and boundary conditions used the NCEP FNL analysis data as well. The model adopted NSSL 2-moment 4-ice scheme for microphysical process, Kain-Fritsch cumulus parameterization scheme, RRTMG long and short-wave radiation scheme, YSU boundary layer scheme and five-layer thermal diffusion land surface scheme. The Kain-Fritsch cumulus scheme was not used for d03 domain. The simulation starts at 12:00 UTC on 22 June and ends at 12:00 UTC on 23 June 2016.

For validating the model result, the ERA5 data, ground radar reflectivity and rain gauge data were used. Figure A2a-f compares the fraction of cloud cover, reflectivity, and rainfall from the WRF model with the observation data. Figure A2a shows the fraction of cloud cover from the WRF model at d02 domain. The cloud area and coverage are consistent with the ERA5 data shown at Fig. A2b. Figure A2c and d compare the reflectivity from the WRF simulation over the d03 domain at 04:00 UTC on June 23 and ground radar at Lianyungang city at 04:02 UTC on June 23, 2016. From radar observation, we can see that the strong echo area is relatively scattered, generally trending from northwest to southeast, and the maximum reflectivity is about 55 dBZ. In the simulation, the strong radar echo is mainly distributed along the northwest-southeast; the radar echo structure and echo intensity are close to the radar observation. Figure A2e and f show the 6-hour accumulated rainfall from 00:00 to 06:00 on June 23 from the WRF model and rain gauge data, respectively. The rainfall covers most areas in the north of Jiangsu Province, and there are two heavy rainfall centers of more than 100mm. The rainfall area in the simulation is similar to that from rain gauge data, and three heavy rainfall centers can be seen in the model result. The maximum rainfall from rain gauge data is approximately 120 mm and maximum from WRF is approximately 126 mm. The amount, scope, and distribution of rainfall from WRF simulation are generally consistent with the rain gauge data. The main difference is in the strong rainfall location and extreme value. Considering the model limitations, the comparison results show that the model captured the convective precipitation process.

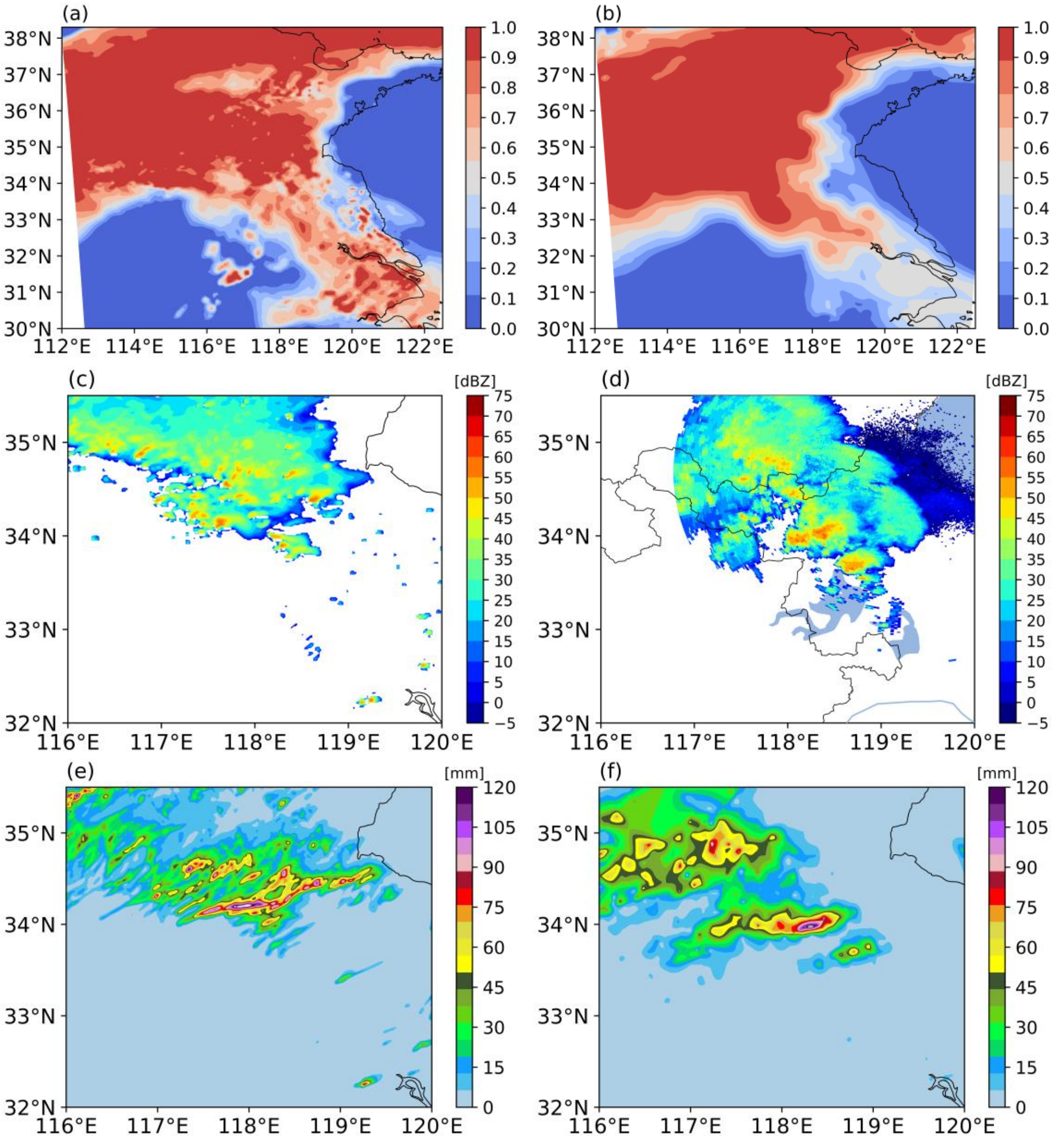

Figure A2: Comparison between the WRF model result and observation data for the convective case. (a) Fraction of cloud cover from the WRF model, (b) fraction of cloud cover from the ERA5 data, (c) radar reflectivity from the WRF model at 04:00 UTC, (d) radar reflectivity observed by the Lianyungang radar at 04:02 UTC, 23 June, (e) WRF model-simulated 6h accumulated rainfall from 0:00 to 06:00 UTC, 23 June, (f) 6h accumulated rainfall from rain gauge data from 0:00 to 06:00 UTC, 23 June 2016."

Particle shape and orientation:

1) **The authors rely on a set of "soft" (mixture of ice and air) particle shapes to evaluated sensitivities to particle shape and orientation. The shapes are spheres and spheroids for snow and rain, and cylinders are additionally included for cloud ice. The T-matrix method is used to calculate scattering properties. It is very unlikely that soft ice spheres and spheroids provide adequate results for evaluating sensitivities to particle shape and orientation for snow or cloud ice at W-band. More realistic variations in particle shapes (e. g., Wood et al., 2015, JAMC) using the discrete dipole approximation for scattering properties can give backscatter cross-sections that vary by a couple of orders of magnitude at larger particle sizes. This seems inconsistent with the results in Figure 6. I request that the authors look at more realistic backscattering cross-sections, particularly for snow, and reexamine their conclusions. These backscattering properties are readily available, from either the Liu database or OpenSSP described in my specific comments below, for example.**

Response: Thanks very much for your valuable suggestion. We have recalculated the scattering properties for cloud ice and dry snow using T matrix and DDA, respectively. Figure 6 has been updated. "

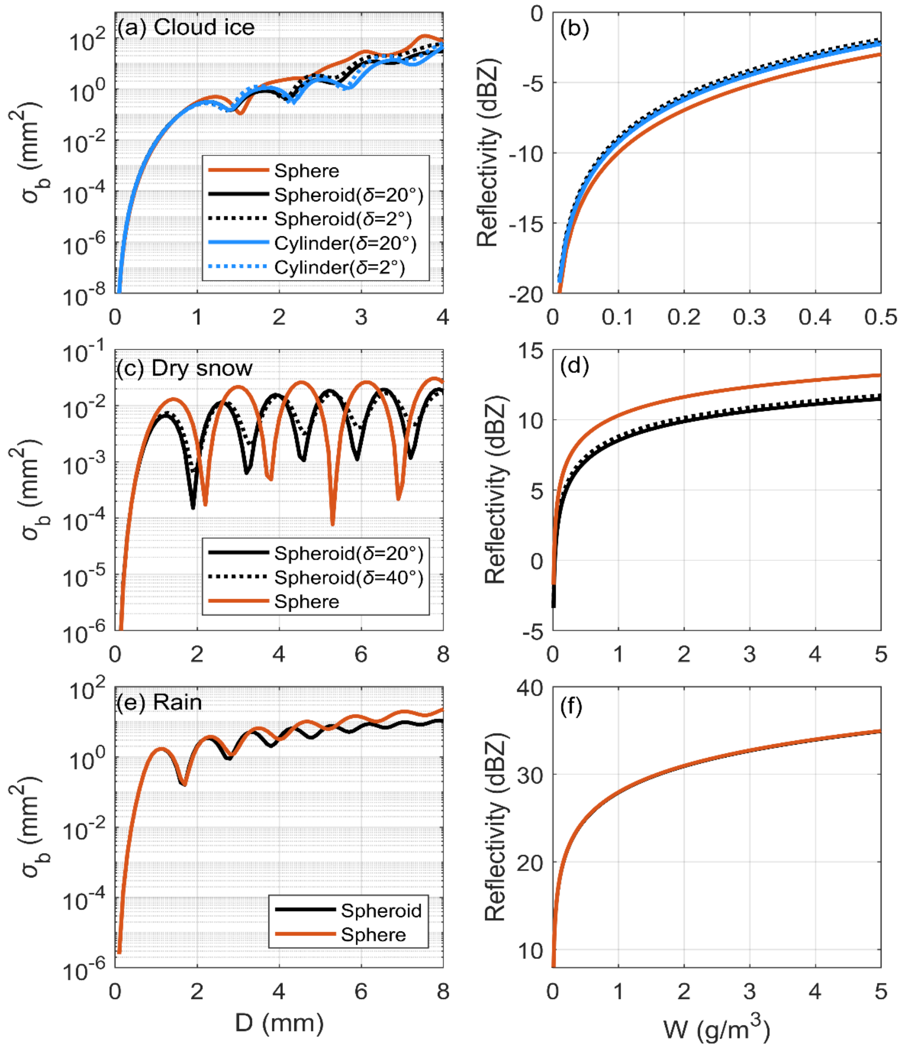

Figure 6: Backscattering cross-section and corresponding radar reflectivity under different shapes for cloud ice, dry

snow, and rain. (a) Comparison of the backscattering cross-sections of ice crystals as spheres, spheroids, or cylinders, where δ is the SD of the canting angle. (b) Radar reflectivity comparison for particles in (a), where the PSD was assumed as a Gamma distribution constrained by Eqs. (7)–(9), with μ=1 and T = –60º C. (c) Comparison of the backscattering cross-sections for dry snow with spheres and spheroids. (d) Radar reflectivity comparison for particles in (c), where the PSD was assumed as an exponential distribution with $N_0 = 3 \times 10^3$ m^{-3} mm^{-1}. (e) Comparison of backscattering cross-sections for raindrops with spheres and spheroids. (f) Radar reflectivity comparison for particles in (e), where the PSD was assumed as a Gamma distribution with $D_0 = 1.25$ mm and μ=3.

The solid and dotted lines in Fig. 6a indicate that the SD of the canting angle (δ) is 2º and 20º, respectively. The backscattering difference for cloud ice was evident between the sphere and non-sphere when the diameter was greater than 1 mm. The radar reflectivity factor in Fig. 6b was obtained with the constrained PSD parameter (section 2.2.3) of T = –60 ºC and μ=1, and the maximum diameter was calculated according to Eq. (8) that was within 0.4 mm. Figure 6b shows that the spherical and non-spherical assumption for cloud ice may result in an average reflectivity difference by approximately 8 %. Figure 6c shows the backscattering cross-section of dry snow with a mass-diameter relation of m=0.0075$D^{2.05}$ (Matrosov et al., 2007; Moisseev et al., 2017), where the axis ratio of the spheroid was 0.6 and the SD of the canting angle was assumed to be 20º and 40º, respectively. When calculating the radar reflectivity factor, the corresponding exponential distribution parameter was $N_0 = 3 \times 10^3$ m^{-3} mm^{-1} and the reflectivity difference between the sphere and spheroid can reach approximately 1.6 dB."

The results in Matrosov (2007) and Wood et al (2015) showed that the reflectivity difference for dry snow between the sphere and spheroid assumption can reach approximately 2 dB. The magnitude of backscattering cross-section and reflectivity difference between spherical and non-spherical in Fig. 6 are basically consistent with those in Matrosov (2007) and Wood et al (2015). The slight difference is mainly due to the different setting of the SD of the canting angle.

In our study, the scattering characteristics of cloud ice (composed of pure ice) and dry snow (composed of ice and air) are calculated separately, as shown in Fig.6. For comparison, Figure R1 shows the backscattering cross-sections for ice and dry snow with spheres (Rayleigh spheres and Mie spheres) and spheroids (axis ratio of 0.6). The result is consistent with that in Wood et al (2015), but more particle shapes were included in Wood et al (2015). We mainly considered the difference between sphere and spheroid with different orientations in this study. In future research, we will consider the influence of more particle shapes on radar reflectivity.

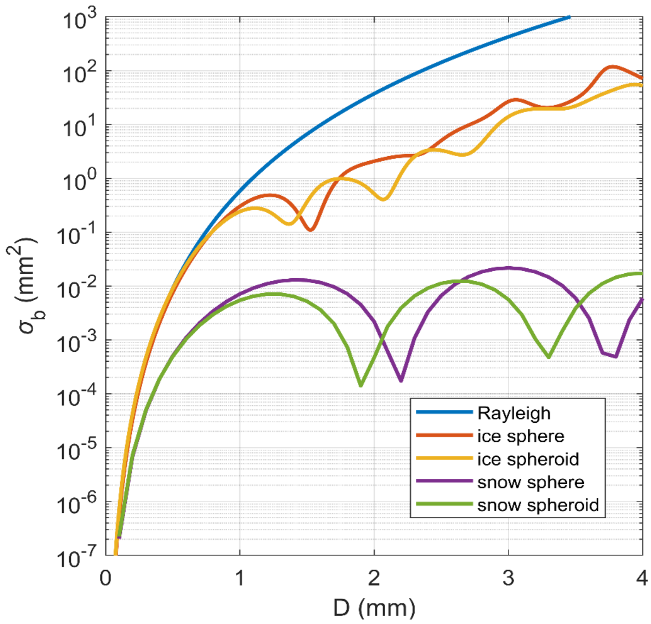

Figure R1: Backscattering cross-sections for solid ice and dry snow (a mass-diameter relation of m=0.0075$D^{2.05}$ was used for dry now), where blue line represents Rayleigh sphere for solid ice, red line represents Mie sphere for solid ice, orange line represents spheroid with axis ratio of 0.6 for solid ice, purple line represents Mie sphere for dry snow, and green line represents spheroid with axis ratio of 0.6 (SD of canting orientation of 20°) for dry snow.

The backscattering cross-sections from T-matrix and DDA were compared as well (the Liu database were not used, because we cannot access the download link). Figure R2 shows the backscattering cross-sections for dry snow with T-matrix and DDA method. The result shows that the scattering properties from T-matrix is similar to those from DDA if the particles are with similar shape assumption.

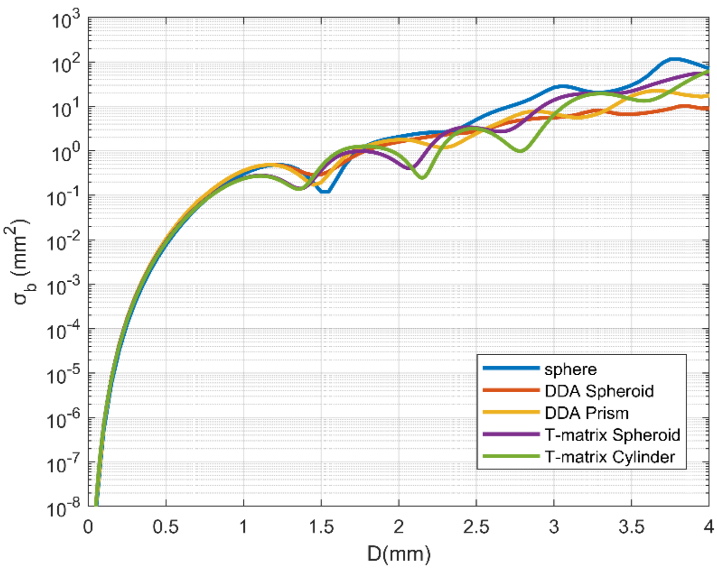

Figure R2: Comparison of backscatter cross-sections for dry snow with T-matrix and DDA method, where blue line represents sphere, orange line represents spheroid with DDA algorithm, yellow line represents hexagonal prism with DDA algorithm, purple line represents spheroid with T-matrix algorithm, and green line represents circular cylinder with T-matrix algorithm.

Specific comments:

L 36-37: I'm not sure why you would say that the CPR is the "most typical spaceborne radar". There are and have been several other spaceborne radars, none of which are cloud radars like the CPR, but rather precipitation radars.

Response: Sorry for the inaccurate expression. The sentence has been rewritten.

"The most widely used spaceborne cloud radar is the millimeter wave cloud profiling radar (CPR) carried onboard the CloudSat satellite (Stephens et al., 2008; Tanelli et al., 2008)."

L 41-42: I also don't understand here why you would say "comprehensive view" and "fully detecting clouds and associated precipitation". There are numerous limitations in terms of spatio-temporal sampling and in measurement capabilities that make the CPR observations incomplete.

Response: Sorry for the unclear description. The sentence has been rewritten.

"This provides an opportunity to advance the understanding of the way water cycles through the atmosphere, by jointly observing clouds and associated precipitation (Behrangi et al., 2013; Ellis et al., 2009; Hayden et al., 2018)."

L 43-45: How does initiating research demonstrate detection capability?

Response: Sorry for the inaccurate statement. The sentence has been rewritten.

"Recently, many countries have begun research on next-generation spaceborne cloud radar (Battaglia et al., 2020; Illingworth et al., 2015; Tanelli et al., 2018; Wu et al., 2018), such as the CPR on the EarthCARE satellite and dual-frequency cloud radar on the Aerosol/Clouds/Ecosystem (ACE) mission (Illingworth et al., 2015; Tanelli et al., 2018)."

L 53-54: Note that "GPM" is the acronym for the project. The relevant instrument is the "Dual-frequency Precipitation Radar", "DPR".

Response: Yes. Thanks for pointing out. The "GPM satellite simulation" has been modified to "Global Precipitation Measurement (GPM) satellite simulator".

L 56-57: The seriousness of the effects of particle shape and orientation depend very much on radar wavelength. The effects on Ka- and Ku-band radars like the DPR are much less than those on the W-band CPR.

Response: Yes, the effects on Ka- and Ku-band radars like the DPR are much less than those on the W-band CPR. Sorry for the inaccurate expression. Thanks for the comment. The sentence has been rewritten. "The radar reflectivity for the W-band is also sensitive to microphysical parameters like the particle size distribution (PSD) model and parameter, particle shape, orientation, and mass".

L 57-58: It is not clear what is meant by "density of mixed particles" here. Does "density" mean the particle concentration, or the actual bulk density of individual particles? Does "mixed particles" mean "mixed-phase particles"? And how does this "density of mixed particles" impact PSD? Where are your citations for these statements?

Response: Sorry for the unclear description. The density here refers to the density-diameter relationship of snow/graupel. The relevant sentences have been rewritten.

"However, the particle shape, composition, orientation, and mass relation all affect the scattering characteristics. The radar reflectivity for the W-band is also sensitive to microphysical parameters like the particle size distribution (PSD) model and parameter, particle shape, orientation, and mass (Mason et al., 2019; Sy et al., 2020; Wood et al., 2013; Wood et al., 2015). A sensitivity analysis is essential for estimating the effects of these uncertainties on simulated radar reflectivity, and guiding appropriate parameter setting in forward modeling."

L 65: What does "optimization physical parameter settings" mean?

Response: Sorry for the unclear description. The "optimization" has been modified to "appropriate".

L 73-246: There is a significant omission of citations to relevant reference material throughout this section. Please examine this section and add citations to appropriate references to support the assumptions you have made.

Response: I am very sorry for the carelessness. Thanks very much for pointing out. The citations in section 2 have been added now in the revised manuscript. Also, we have checked the references and citations one by one throughout this manuscript.

L 77-78: What makes the cases you selected "typical"? Were the cases really selected by going through the historical CloudSat data? Were there any other criteria? Why did you choose the particular cases presented in sections 4.1 and 4.2?

Response: The cases were selected by combining historical CloudSat data and typical weather processes observed on the ground. For example, the stratiform case in section 4.1 was a large-scale low trough cold front cloud system in northwest China. The weather process covered a large area and lasted for a long time. Many Chinese scholars have simulated and studied the weather process (Liu et al., 2015; Sun et al., 2015). The convective case in section 4.2 was a large-scale severe convective weather process that occurred in the Lower Yangtze-Huaihe river on June 23, 2016. This deep convective process caused strong wind, hail and rainstorm in Jiangsu province (Kuang et al., 2018).

Liu, T., Sun, J., Zhou, Y.Q., Peng, C., and Yan, F.: A simulation study on through cold front cloud structure (in Chinese), Meteorological Monthly, 41: 1-13, 2015, doi:10.7519/j.issn.1000-0526.2015.10.006.

Sun, J., Yang, W.X., Zhou, Y.Q.: Numerical simulations of cloud structure and seed ability of a precipitation stratiform in Hebei (in Chinese), Plateau Meteorology, 34: 1699-1710, 2015, doi:10.7522/j.issn.1000-0534.2014.00086.

Kuang, X., Yin, Y., Chen J.H., and Xiao, H.: Simulation analysis of strong convective weather processes in Huanghuai River based on WRF model and CloudSat satellite data (in Chinese). Journal of the Meteorological Sciences, 38:331-341, 2018, doi:10.3969/2017jms.0035.

L 79-80: How were the WRF simulation results verified by observation data? The validation

of the model results probably deserves a section of its own.

Response: Thanks very much for your valuable suggestion. The model validation was provided in Section 4.1.1. More validation results have been added in Appendix A. Detailed information are in the response to "overall comments: WRF model simulations".

L 77-85: This is a very cursory description of the methodology for the simulations. It is missing many relevant details about the setup of the model. What microphysics parameterization was used?

Response: Thanks very much for the suggestion. Detailed description of the model setup has been added in Appendix A.

"The simulation for this stratiform case was conducted with four nested grids (d01, d02, d03, and d04), and the inner domain was centered at 41.08°N, 117.61°E. The horizontal grid spacings are 27km, 9km, 3km, and 1km and the corresponding grids are 120×120, 180×180, 300×300, and 300×300. The vertical resolution increases with height from approximately 50 m near the surface to 600 m near 50 hPa. Time steps of 180s and 6.67s were used for d01 domain and d04 domain, respectively. The 6-hourly NCEP FNL operational global analysis data on 1° × 1° grids were used to provide the initial and boundary conditions. In term of physical scheme, the model adopted CAM 5.1 5-class scheme, Grell-Freitas cumulus parameterization scheme, RRTM long and short-wave radiation scheme, YSU boundary layer scheme, Monin-Obukhov surface layer scheme and thermal diffusion land surface scheme. The cumulus parameterization scheme was used for d01 and d02 domains only."

L 97-98: Because contact freezing is essentially instantaneous, I think graupel are usually considered to be ice-air mixtures unless they fall below the freezing level and begin melting.

Response: Sorry for the incorrect statement. Thank you for pointing out. The sentence has been rewritten. "Dry snow and graupel are a mixture of air and ice, while wet snow and graupel are a mixture of air, ice, and water."

L 100-101: Is there a reason to use Maxwell-Garnett rather than something like a three-component Bruggeman model (e.g., Haynes et al. 2009, JGR Atmosphere). Also, note that it is "Garnett" rather than "Garnet".

Response: Bruggeman model can also be used. In this study, we use Maxwell-Garnett model.

Thanks very much for pointing out. "Garnet" has been revised to "Garnett".

L 109: I think this formula is correct only if mu=0. See, e.g., Chase et al. (2020, Atmosphere), equations 7 and 9.

Response: Yes, this formula is correct only if μ=0. Thank you very much for pointing out. This formula has been revised to

$$N_w = \frac{W}{\pi\rho_w}\left(\frac{4(3.67+\mu)}{(4+\mu)D_0}\right)^4 \quad (2)$$

L 114: More correctly, R_gas is the specific gas constant. If you are using the R_gas for dry air and T is the air temperature, this formula is not correct.

Response: Sorry for the incorrect expression. Thank you for pointing out. The formula has been revised.

$$W = \frac{P}{R_g T_V} * 1000 * q \ , \qquad (3)$$

where R_g is the specific gas constant, P is the air pressure in hPa, T_V is the virtual temperature in K, q is the mixing ratio of the hydrometeor based on the WRF output in kg/kg, and the units of W are g/m^3.

L 127-129: Was there a reason for using the normalized gamma distribution rather than making the more common assumption of a negative exponential distribution?

Response: In this study, we used the normalized gamma distribution for raindrop and cloud water. For raindrop and cloud water, the three-parameter gamma distribution is more general form of DSD compared with the exponential distribution with two variables (Ryzhkov and Zrnic, 2019; Zhang, 2017).

L 131-133: Cloud ice particle habit also depends on the amount of supersaturation in the environment where the particle forms and grows. The more common term for "collision and merging" is "aggregation".

Response: Thanks very much for your suggestion. The sentence has been rewritten. "Cloud ice is mainly composed of various non-spherical ice crystals; the size and shape of ice crystal particles are complex and diverse, depending on the cloud temperature, the degree of supersaturation in the environment where the particle forms and grows, and whether the particles have experienced aggregation processes in the cloud (Heymsfield et al., 2013; Ryzhkov and Zrnic, 2019)."

L 133-134: Is the Liu database relevant to this work? Was it used in some way? The next sentence states that T-matrix calculations were used, not the Liu database scattering properties.

Response: The database in Liu (2008) included the scattering characteristics of ice crystals, but it was not used in our study (we cannot access the download link). Here, we used the T-matrix to calculate the scattering properties of hydrometeor particles.

L 136: I don't find this Hogan et al. citation in the bibliography. How was D defined for these ice particles? Is it an equivolume ice diameter?

Response: I am very sorry for the careless. Hogan et al. citation has been added now in the bibliography. Here D refers to the larger dimension of cylinder. The D in this formula has been revised to L to be distinguished from the equivalent volume diameter in other formulas.

$$\begin{cases} L/h = 5.068L^{0.586} & L > 0.2\,mm \\ L/h = 2 & L \le 0.2\,mm \end{cases} \qquad (5)$$

Hogan, R.T., Tian, L., Brown, P.R.A., Westbrook, C.D., Heymsfield, A.J., and Eastment, J.D.: Radar scattering from ice aggregates using the horizontally aligned oblate spheroid approximation, J. Appl. Meteorol. Climatol., 51, 655-671, doi: 10.1175/JAMC-D-11-074.1, 2012.

L 137: The Fu, 1996 reference cited here is not in the bibliography. Please include it. Were these circular cylinders or hexagonal cylinders? Can you also provide a reference that describes the T-matrix method or code that was applied?

Response: I am very sorry for the careless. Thanks very much for pointing out. Fu (1996) has been added in the references. These were circular cylinders. Mishchenko and Travis (1998) has been added to describe the T-matrix method.

Fu, Q.: An accurate parameterization of the solar radiative properties of cirrus clouds for climate models, J. Climate, 9, 2058-2082, doi: 10.1175/1520-0442(1996)009<2058:APPOTS>2.0.CO;2, 1996.

Mishchenko, M.I., and Travis, L.D..: Capabilities and limitations of a current FORTRAN implementation of the T-matrix method for randomly oriented, rotationally symmetric scatterers, J. Quant. Spectrosc. Radiat. Transfer, 60, 309-324, doi: 10.1016/S0022-4073(98)00008-9, 1998.

L 139: I'm not sure what point this sentence is making. Perhaps try to state it more clearly. To me, it seems the distribution of orientations is an inherent part of the "falling behavior".

Response: Sorry for the unclear statement. This sentence has been rewritten. "Distribution of orientations of ice particles depends on their falling behavior. According to Melnikov and Straka (2013), we assume that the ice crystal orientations follow a Gaussian distribution, with a mean canting angle of 0° and a SD between 2° and 20°."

L 142: I don't believe that cloud ice size distributions are considered similar to those of raindrops. Do you have references that suggest an exponential distribution is appropriate for cloud ice?

Response: In this study, the normalized gamma distribution was adopted for cloud ice, which was according to the empirical fits derived in Heymsfield et al (2013).

Heymsfield, A. J., Schmitt, C., and Bansemer, A.: Ice cloud particle size distributions and pressure-dependent terminal velocities from in situ observations at temperatures from 0^{o} to -86^{o}C, J. Atmos. Sci., 70, 4123-4154, doi: 10.1175/JAS-D-12-0124.1, 2013.

L 144: Same comment as I made above regarding L 109.

Response: Thanks very much for pointing out. The formula has been revised.

L 156: The term "aggregation" is more typically used, rather than "conglomeration".

Response: Thanks very much for your suggestion. This sentence has been rewritten. "Snowflakes are usually formed by the aggregation and growth of ice crystals."

L 157-159: Be cautious about using the terms "typically" or "normally", here and in other

places in the paper. Is it reasonable to say that some value is typical or normal when only one or two supporting citations are provided?

Response: Thanks for your suggestion. The terms "typically" and "normally" have been removed from the corresponding sentences.

L 162-168: How is D defined for the snowflakes? The long axis of the assumed spheroid or the equivolume spherical ice diameter?

Response: *D* is the volume equivalent diameter. This has been added in the revised manuscript.

L 171: The correct name for the second citation is "von Lerber et al."

Response: Thanks very much for pointing out. "von et al" has been revised to "von Lerber et al".

L 177-178: OK, this describes the "D" for the mass and density relations, but it still isn't clear what diameter was used.

Response: Sorry for unclear description. Thank you for pointing out. The sentence has been rewritten. "In this study, the diameters in the mass and density relations were converted to the volume equivalent diameter *D* according to the assumed axis ratio."

L 188: What is "mass water fraction"? Most of the mass of a graupel particle is due to water (in the form of ice) so the mass fraction of that water will almost always be near 1.0 since the mass of air in the graupel particle is very small.

Response: Sorry for the inaccurate statement. The mass water fraction is for wet graupel. The sentence has been rewritten to make it clear. "Here the shape of graupel was modeled as a spheroid, where the axis ratio for dry graupel was set to a constant value of 0.8, and the axis ratio for melting graupel was modeled according to Ryzhkov et al. (2011)."

L 200-203: Are you also ignoring aggregation and collision-coalescence?

Response: Yes, the aggregation and collision-coalescence were ignored as well. "Neglecting aggregation, collision-coalescence, evaporation, and the small amount of water that may collect on the particle owing to vapor diffusion, we assumed that the mass of snow was conserved during the evolution process from dry snow, to wet snow to liquid water."

L 209-211: But the exponent "b" changes as the particle melts and the shape of the particle melts, does it not? In the end, when the particle is fully melted, and nearly spherical, the value of "b" should be near 3. Can you justify using b=2.1 over the full range of particle melting?

Response: Yes, the value of "b" varies with the melting degree. Sorry for the unclear description. With an assumed f_w value, the density of wet snow can be calculated from Eq. (16). Then, the density parameter (prefactor "a" or exponent "b") can be obtained according to the density-diameter relationship. The sentence has been rewritten. "The density parameter in Eq. (11) can be obtained according to the density-diameter relationship, where the density is calculated from Eq. (16) with an assumed f_w value."

L221: Should the left hand side of equation 19 be "N_w(D_w)"?

Response: Yes. Thanks for pointing out. The equation 19 has been rewritten.

$$N_w\left(D_w\right) = N_{ms}\left(D_{ms}\right)\frac{3}{b}\left(\frac{6}{\pi}a\right)^{-\frac{1}{3}} D_{ms}^{\frac{3-b}{3}}, \tag{19}$$

L 235: Usually the term "extinction cross-section" is used.

Response: Thanks for your suggestion. The term "extinction section" has been revised to "extinction cross-section".

L 239-241: And how were the attenuation and the two-way path integrated attenuation addressed when combining different types of hydrometeors?

Response: The relevant information has been added now in the revised manuscript. "If there are many types of hydrometeors at the same height, the equivalent unattenuated radar reflectivity and attenuation coefficient of each hydrometeor is calculated based on the look-up table. Then, the total unattenuated radar reflectivity at this height is obtained by adding all types of hydrometeors, and the two-way attenuation is obtained by integrating the total attenuation coefficient with path. The attenuated radar reflectivity is obtained by subtracting the attenuation from the unattenuated radar reflectivity."

L 247-333: This is a general comment for the sensitivity section. Wood and L'Ecuyer (2021, AMT) looked at W-band retrieval uncertainty sources. How do your results compare with theirs?

Response: Thanks very much for your valuable suggestion. Wood and L'Ecuyer (2021) showed that the contributions to uncertainties in W-band radar reflectivity from the particle model parameters (e.g., the coefficients and exponents of the mass relationships) was most substantial, which may cause 5 to 15 dB reflectivity uncertainty. Our study shows that he reflectivity change caused by variation in prefactor *a* from 0.005 to 0.013 g/cm^b for snow and 0.02 to 0.06 g/cm^b for graupel (*W* remains constant) can reach 7–10 dB. The reflectivity change caused by variation in *b* was approximately 0.5-2 dB. The mass relationships cause substantial uncertainties in W-band radar reflectivity. Our results are consistent with those in Wood and L'Ecuyer (2021). The comparison with Wood and L'Ecuyer (2021) has been added in the revised manuscript.

"In all, the mass relationships that depend on particle habits and formation mechanisms, cause substantial uncertainties in W-band radar reflectivity. Our results are consistent with the sensitivity analysis by Wood and L'Ecuyer (2021) who pointed out that the W-band radar reflectivity uncertainty for snowfall was dominated by the particle model parameter (e.g., the prefactors and exponents of the mass relationships). This relationship can cause the reflectivity uncertainty of several to more than 10 dB. The results indicate that improved constraints on assumed particle mass models would improve forward-modeled radar reflectivity and physical parameter retrieval."

L 258: It's probably more correct to say that the particles are small "compared to the radar

wavelength".

Response: Thanks for your suggestion. The sentence has been rewritten. "Cloud water particles are small compared to the radar wavelength, which is in the linear growth stage in the Mie scattering region."

L 259-261: Check grammar/sentence structure.

Response: Sorry for poor writing. The sentence has been rewritten. "With a five-fold increase in D_0 (W remains constant), e.g., increasing from 10 to 50 μm, the reflectivity increases by approximately 20 dB."

L 259-264: Were these sensitivities calculated by perturbing D_0 while simultaneously keeping W constant? Or did W increase as D_0 was increased?

Response: These sensitivities were calculated by perturbing D_0 while simultaneously keeping W constant.

L 265: Please check this equation reference. I think it is not correct.

Response: This equation does not cite references. The references are for the value of μ.

$$N_t = \int_0^{D_{max}} N(D)dD \tag{9}$$

Owing to the monotonicity of the functions, D_0 can be solved numerically. For cloud ice, μ usually ranges from 0 to 2 (Tinel et al., 2005; Yin et al., 2011).

L 278: This isn't the correct equation to convert N_0 to dB(N_0). "dB" indicates "decibel" (i.e., "deci" "Bel", or one-tenth of a Bel). dB(N_0) should be 10*log10(N_0).

Response: Sorry for the unclear exhibition. Here, we use $dBN_0 = log_{10}(N_0)$ to convert N_0 of 10^3 to 3 just for the convenience of writing and image display. We don't convert N_0 to decibel.

L 280-282: This states "may result in an uncertainty of approximately 45% and 30% for snow and graupel", but it doesn't say what property of the snow and graupel this uncertainty applies to. Please clarify.

Response: Thanks very much for your valuable comment. We have added the description of the cause of reflectivity uncertainty contributed by "a" variation. "The mass power-law parameters vary with snow/graupel type, shape, and porosity. An increase in *a* lead to an increase in the corresponding particle scattering properties. The intercept parameter N_0 will slightly decrease with the increase in *a* implicitly representing the effects of aggregation at warmer temperatures (Woods et al., 2008). Among them, the change to particle scattering properties caused by the perturbation of *a* play a dominant role in the reflectivity change. Using an average mass-power relation assumption, the variation in *a* as a result of the degree of aggregation and riming, and particle shapes may result in the reflectivity uncertainty of approximately 45 % and 30 % for snow and graupel, respectively."

L 296-299: Please recheck your values for D_0. 20 mm and 30 mm seems extremely large for liquid cloud droplets. Either there is a typographic error here, or an error in the

calculation of D_0, I think.

Response: Sorry for the careless. This is a typographic error. Thanks very much for pointing out. 20 mm and 30 mm has been revised to 20 μm and 30 μm.

L 297-299: I don't think there is much gained by including the results from the Gamma(D_0=30) case. Clearly, if two PSDs for liquid water droplets are nearly the same, the simulated reflectivities will be nearly the same. The significant point here is that, given the same water content, different assumptions about the shape of the PSD can have a strong effect on the simulated reflectivity.

Response: Thanks very much for your valuable suggestion. This gamma case (D_0=30 μm) really doesn't make much sense. The case of gamma D_0=30 μm has been removed.

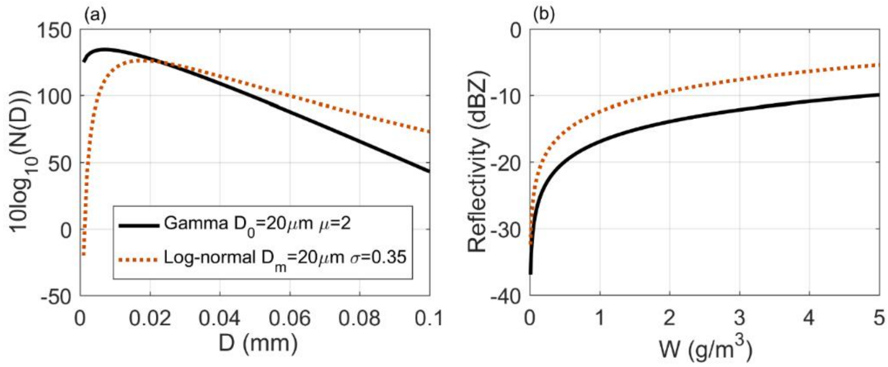

Figure 5: Impact of PSD models on radar reflectivity for cloud water. (a) Black solid line is for the gamma distribution: $W = 1$ (g/m^3), $D_0 = 20\ \mu m$, and $\mu = 2$. Red-dotted line is for the log-normal distribution: $W = 1\ g/m^3$, $D_m = 20\ \mu m$, and $\sigma = 0.35$. (b) Variation in the radar reflectivity with W and the PSD models, where the PSD models are from (a).

L 300: It's probably more correct to say the "reflectivity change" was 4.5dB.

Response: Thanks very much for your suggestion. The sentence has been rewritten. "The reflectivity change caused by the different PSD models was approximately 4.5 dB."

L 314-334: I think it's questionable whether these different shapes of soft (mixtures of ice and air) particle shapes give a good representation of the sensitivity of reflectivity to particle shape and orientation. Methods such as the discrete dipole approximation are accepted as giving much more realistic values for backscattering by ice and snow particles. I think it would be appropriate to look at other sources of DDA backscattering properties (e.g. the Liu database mentioned earlier, or OpenSSP) to see if your results are consistent with DDA results.

Response: Thanks very much for your valuable suggestion. We have recalculated the scattering properties for cloud ice and dry snow using T matrix and DDA algorithm, respectively. Figure 6 has been updated. Detailed information can be seen in the response to the "overall comments: particle shape and orientation".

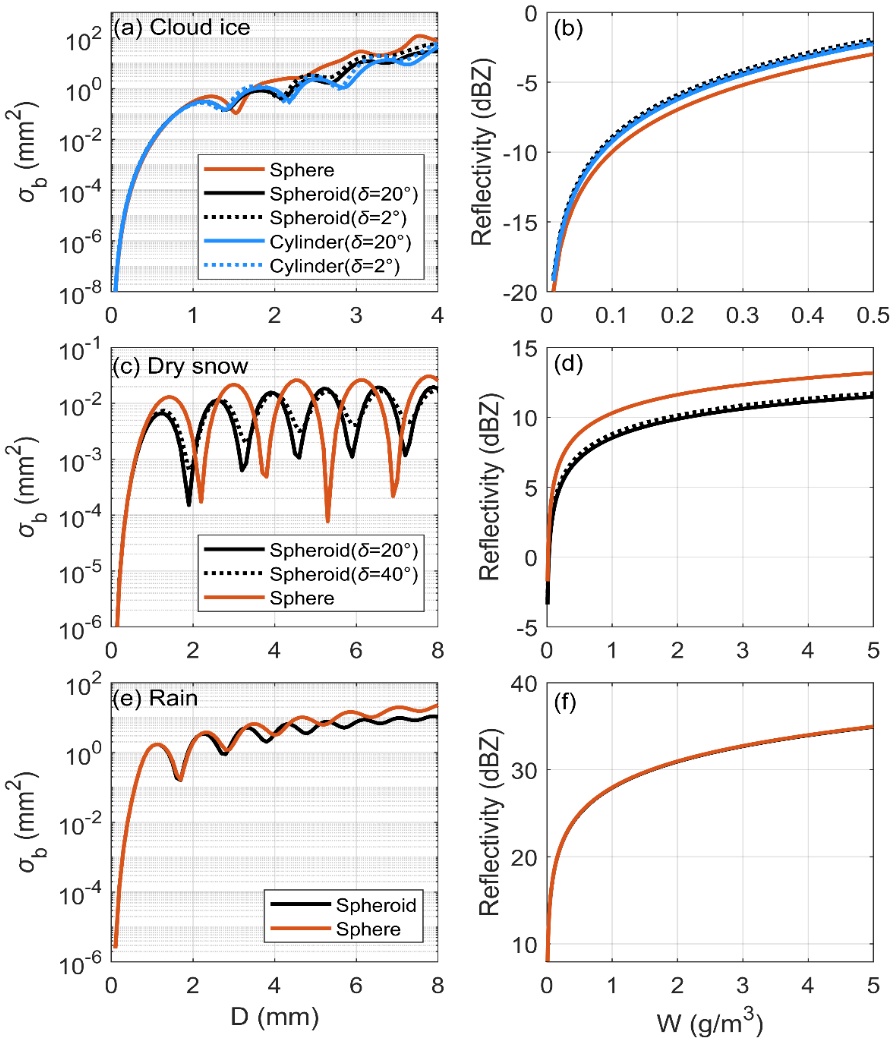

Figure 6: Backscattering cross-section and corresponding radar reflectivity under different shapes for cloud ice, dry snow, and rain. (a) Comparison of the backscattering cross-sections of ice crystals as spheres, spheroids, or cylinders, where δ is the SD of the canting angle. (b) Radar reflectivity comparison for particles in (a), where the PSD was assumed as a Gamma distribution constrained by Eqs. (7)–(9), with μ=1 and T = –60º C. (c) Comparison of the backscattering cross-sections for dry snow with spheres and spheroids. (d) Radar reflectivity comparison for particles in (c), where the PSD was assumed as an exponential distribution with $N_0 = 3 \times 10^3$ m^{-3} mm^{-1}. (e) Comparison of backscattering cross-sections for raindrops with spheres and spheroids. (f) Radar reflectivity comparison for particles in (e), where the PSD was assumed as a Gamma distribution with $D_0 = 1.25$ mm and μ=3.

The results in Matrosov (2007) and Wood et al (2015) showed that the reflectivity difference for dry snow between the sphere and spheroid assumption can reach approximately 2 dB. The magnitude of backscattering cross-section and reflectivity difference between spherical and non-spherical in Fig. 6 are basically consistent with those in Matrosov (2007) and Wood et al (2015). The slight difference is mainly due to the different setting of the SD of the canting angle.

L 345-346: What was the vertical grid spacing? Was the spacing uniform or stretched (with layers getting generally thicker with height)? What data were used for initial and boundary conditions? What time-stepping was used? What microphysical parameterizations were used?

Response: Thanks for the comment. The detailed description of model setup has been added in the Appendix A.

"The simulation for this stratiform case was conducted with four nested grids (d01, d02, d03, and d04), and the inner domain was centered at 41.08°N, 117.61°E. The horizontal grid spacings are 27km, 9km, 3km, and 1km and the corresponding grids are 120×120, 180×180, 300×300, and 300×300. The vertical resolution increases with height from approximately 50 m near the surface to 600 m near 50 hPa. Time steps of 180s and 6.67s were used for d01 domain and d04 domain, respectively. The 6-hourly NCEP FNL operational global analysis data on 1° × 1° grids were used to provide the initial and boundary conditions. In term of physical scheme, the model adopted CAM 5.1 5-class scheme, Grell-Freitas cumulus parameterization scheme, RRTM long and short-wave radiation scheme, YSU boundary layer scheme, Monin-Obukhov surface layer scheme and thermal diffusion land surface scheme. The cumulus parameterization scheme was used for d01 and d02 domains only. "

L 347: It's probably more correct to say "interior domains" rather than "internal layers".

Response: Thanks very much for your suggestion. The term of "internal layers" has been revised to "interior domains".

L 359-360: I'm not sure it's accurate to say that WRF "accurately simulated the cloud system" based only on comparisons of cloud fraction and cloud top temperature.

Response: Besides cloud fraction and cloud top temperature, we have added comparisons of cloud water path (CWP) in Appendix A in the revised manuscript.

Besides the cloud fraction and cloud top temperature shown in Fig. 8, the cloud water path (CWP) from MODIS was used for model result verification as well. Figure A1a is the cloud water path calculated from vertical integration of WRF output cloud water over d01 domain at 03:30 UTC, 25 September, and Fig. A1b is the cloud water path from MODIS Level 2 product at 03:35 UTC, 25 September 2012. The scanning width of MODIS is 2330 km, and the horizontal resolution for the product of CWP is 1 km. The CWP distribution of model result has similar pattern as MODIS observation and the value of CWP are close, but the peaks of the two are slightly offset. Due to the measurement techniques and model limitations, the model simulations may be biased from the observations. However, the distribution, structure, and value of CWP from model and MODIS observation generally agree well.

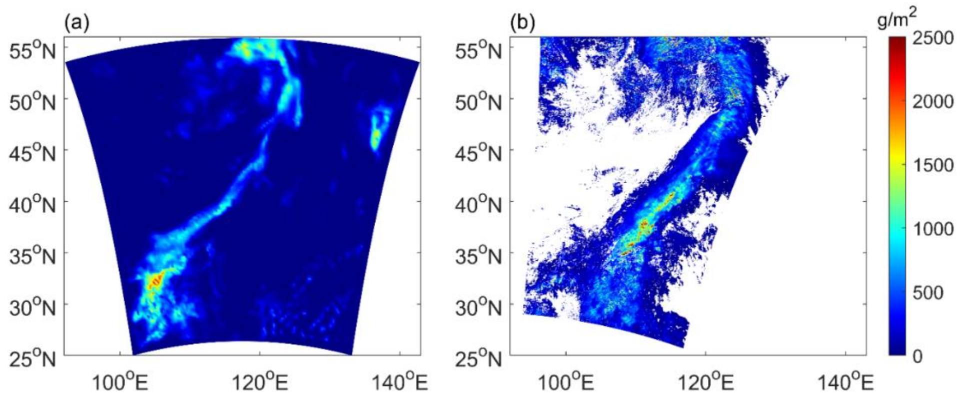

Figure A1: Comparison of CWP between the WRF model result and MODIS data for the stratiform case. (a) CWP from the WRF model at 03:30 UTC, (b) CWP from MODIS observation at 03:35 UTC, 25 September 2012.

L 362-363: I'm not sure that choosing to use the WRF results along the CloudSat track is an effective way to do comparisons between models and satellite observations. One of the frequent errors in models is features like clouds and precipitation may not be located precisely in the location of interest at a particular time. As an example, modeled fronts and their associated precipitation may propagate more slowly or more rapidly than the observed preciptation. Perhaps a better approach would be to statistically compare the properties of the modeled versus the observed clouds and precipitation, using model results from the area under *and near* the CloudSat ground track.

Response: Thanks very much for your valuable comment. Yes, the model result may not be located precisely in the location of interest at a particular time. The area used for validation was much larger than that of CloudSat trajectory, which included the area under and near the CloudSat ground track. Besides, we have added the statistically comparison for the model validation of the convective case.

In Fig.8, the CloudSat track was along the black line in the d04 domain, which was just in the innermost domain. The model validation is for d02 or d01 domain. For the convective case, CloudSat observed this convective process at 04:30 AM on June 23, 2016. In the model validation of convective case, we compared the reflectivity from the WRF simulation over the d03 domain at 04:00 UTC on June 23 and ground radar at Lianyungang city at 04:02 UTC on June 23, 2016. The 6-hour accumulated rainfall data were also compared with those from rain gauge.

"For validating the model result, the ERA5 data, ground radar reflectivity and rain gauge data were used. Figure A2a-f compares the fraction of cloud cover, reflectivity, and rainfall from the WRF model with the observation data. Figure A2a shows the fraction of cloud cover from the WRF model at d02 domain. The cloud area and coverage are consistent with the ERA5 data shown at Fig. A2b. Figure A2c and d compare the reflectivity from the WRF simulation over the d03 domain at 04:00 UTC on June 23 and ground radar at Lianyungang city at 04:02 UTC on June 23, 2016. From radar observation, we can see that the strong echo area is relatively scattered, generally trending from northwest to southeast, and the maximum reflectivity is about 55 dBZ. In the simulation, the strong radar echo is mainly distributed along the northwest-southeast; the radar echo structure and echo intensity are close to the radar observation. Figure A2e and f show the 6-hour accumulated rainfall from 00:00 to 06:00 on June 23 from the WRF model and rain gauge data, respectively. The rainfall covers most areas in the north of Jiangsu Province, and there are two heavy rainfall centers of more than 100mm. The rainfall area in the simulation is similar to that from rain gauge data, and three heavy rainfall centers can be seen in the model result. The maximum rainfall from rain gauge data is approximately 120 mm and maximum from WRF is approximately 126 mm. The amount, scope, and distribution of rainfall from WRF simulation are generally consistent with the rain gauge data. The main difference is in the strong rainfall location and extreme value. Considering the model limitations, the comparison results show that the model captured the convective precipitation process.

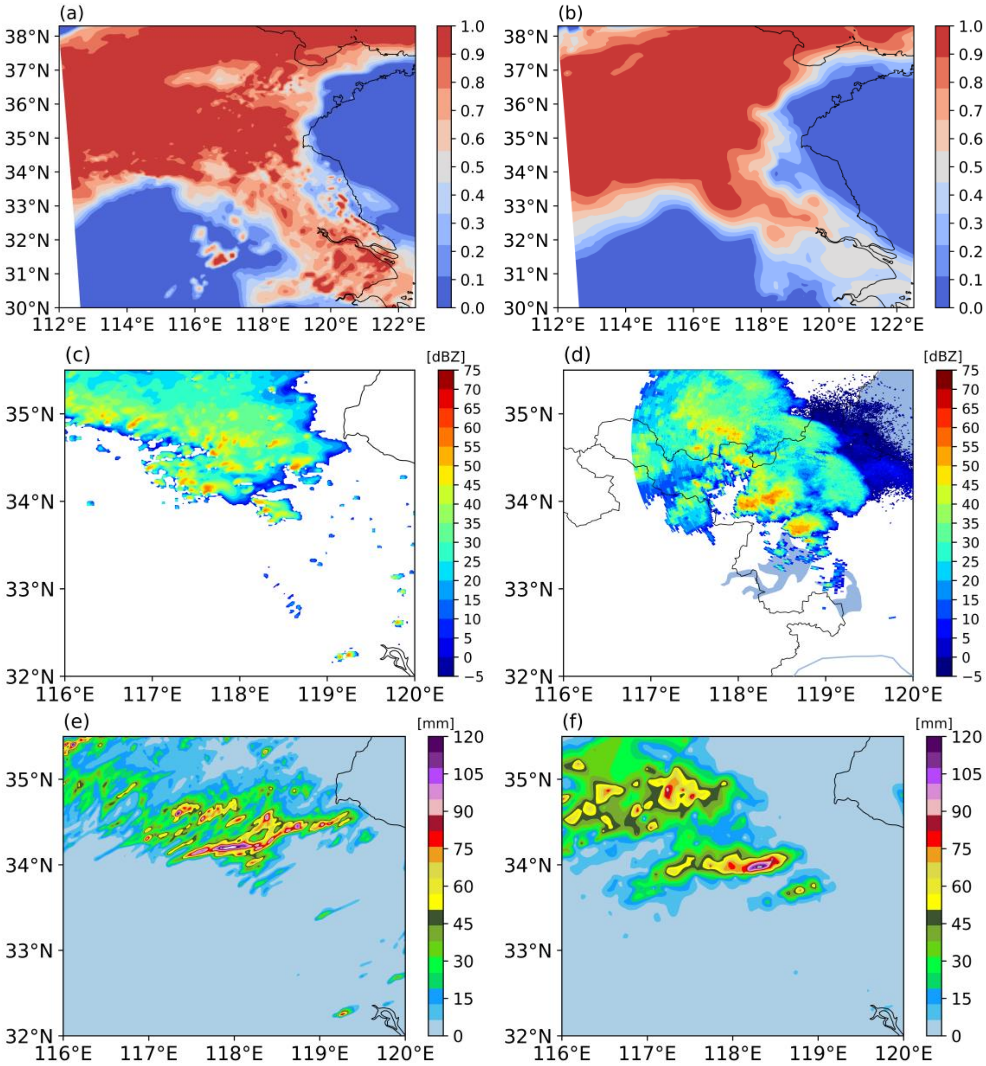

Figure A2: Comparison between the WRF model result and observation data for the convective case. (a) Fraction of cloud cover from the WRF model, (b) fraction of cloud cover from the ERA5 data, (c) radar reflectivity from the WRF model at 04:00 UTC, (d) radar reflectivity observed by the Lianyungang radar at 04:02 UTC, 23 June, (e) WRF model-simulated 6h accumulated rainfall from 0:00 to 06:00 UTC, 23 June, (f) 6h accumulated rainfall from rain gauge data from 0:00 to 06:00 UTC, 23 June 2016."

L 367-369: Regarding "Snow is widely distributed...", can you provide more details? Are you talking about the horizontal extent, the vertical extent, or something else. Maybe

something like "The vertical extent of snow is widely distributed...". Same comment with respect to the next statement, which is about rain. "Rich" is not a clear description. Do you just mean to say the total water contents for cloud water, snow and rain were large?

Response: Sorry for the unclear statement. Thanks very much for your suggestion. The relevant sentences have been rewritten. "The vertical extent of snow is widely distributed, ranging from 3 to 10 km. Rain is mainly below 3 km, with water contents between 0.1 and 0.2 g/m^3. At approximately 0 ºC, the water content for cloud water, snow, and rain were large, which led to a high total water content, with a maximum of 0.57 g/m^3."

L 372: The Yin et al. (2017) work cited here does not appear in the bibliography.

Response: I am very sorry for the careless. Thanks very much for pointing out. The Yin et al. (2017) has been added in the bibliography.

Yin, M.T., Liu, G.S., Honeyager, R., and Turk, F.J.: Observed differences of triple-frequency radar signatures between snowflakes in stratiform and convective clouds, J. Quant. Spectrosc. Radiat. Transfer, 193, 13-20, doi: 10.1016/j.jqsrt.2017.02.017, 2017.

L 375-376: See my comment regarding the Figure 9 caption (L 724). It's probably more clear to refer to these as "unattenuated reflectivities", "attenuation" (is this one-way or two-way?), and "attenuated reflectivities".

Response: Thanks very much for the suggestion. The terms of "reflectivity before attenuation", "attenuation", "reflectivity after attenuation" have been revised to "unattenuated reflectivities", "two-way attenuation", "attenuated reflectivities".

L 379-381: Suggest using "unattenuated reflectivity" and "attenuated reflectivity". Also rather than the "end of the melting region", use "below the melting layer" or "below the melting level." Also suggest using "with attenuation" and "without attenuation" rather than "after attenuation" and "before attenuation". "Before" and "after" can have misleading implications when talking about a radar beam propagating downward through the atmosphere. Finally, there is a well-known reference to this behavior in W-band radar observations from space. See Sassen et al. (2007, Geophysical Research Letters).

Response: Sorry for the unclear expression. Thanks very much for your valuable suggestion. The relevant terms and sentences have been rewritten. "The unattenuated radar reflectivity in the melting layer was equivalent to the reflectivity in the rain region. With attenuation, the radar reflectivity showed a rapid signal decline below the melting layer, and the bright band became evident (Sassen et al., 2007)."

L 382-383: Did you demonstrate this, or did you mean to cite existing work? How large does this diameter need to be, and how is this relevant to the bright band discussion? If I look at figures 6 and 7, the backscatter cross-sections for the larger particles do not appear to be stable.

Response: Sorry for the unclear description. The sentence has been rewritten. "For the 94 GHz radar, the Mie scattering effect was dominant. The raindrops with a diameter less than 1 mm are the dominant contributor to the radar reflectivity profile (Kollias and Albrecht, 2005). Although larger snowflakes melt and produce larger raindrops at depth in the melting layer, their contribution to the reflectivity was not significant, owing to a decrease in their number concentration."

L 396: Usually just "bright band".

Response: Thanks for your suggestion. The term of "brightness band" has been revised to "bright band".

L 399: Rather than using different names for this feature ("brightness band", "bright band", "strong echo band"), please choose one name and use it consistently. Also, when you say the reflectivity was stronger, what are you comparing to?

Response: Thanks very much for your valuable suggestion. The terms of "brightness band", "strong echo band" all have been revised to "bright band". Besides, the sentence about stronger reflectivity has been rewritten. "In Fig.10b, the radar reflectivity below 0 °C was evidently stronger than the echo above 0 °C; the width and location of the bright band were considerably different from the bright band in the simulation with the improved setting and CloudSat observation."

L 400-401: How did you calculate this relative error? Relative errors shouldn't be calculated using "dB" values (i.e. (dB_test - dB_true)/dB_true. The values should be converted back to linear units (e.g., mm^6 m^-3), then the relative error calculated.

Response: Thanks very much for your valuable suggestion. The description of the calculation of relative error has been added. "The trends in the two profiles were basically identical; the relative error ($|Z_{sim} - Z_{obs}| / Z_{obs}$, where Z_{sim} represents the simulated reflectivity and Z_{obs} represents the observations, the units of Z_{sim} and Z_{obs} are converted to mm^6/m^3) at each height was mostly within 15 %."

L 407-408: See my earlier comment concerning the modeling of the stratiform case. Additional details about the model configuration would be interesting to see. What was used for convective parameterization?

Response: Thanks for your suggestion. Detailed description of model setup has been added in the Appendix A.

"For the convective case, three nested grids (d01, d02 and d03) with horizontal grid spacings of 22.5km, 7.5km, and 1.5km and corresponding grid points of 70×70, 126×126, and 280×280 were used for the convective case simulation. The inner domain d03 is centered at 34.02°N, 118.20°E. A total of 39 vertical layers with stretch spacing from the surface to 50 hPa were used, with time steps of 90, 30, and 6 s for d01, d02 and d03, respectively. The initial and boundary conditions used the NCEP FNL analysis data as well. The model adopted NSSL 2-moment 4-ice scheme for microphysical process, Kain-Fritsch cumulus parameterization scheme, RRTMG long and short-wave radiation scheme, YSU boundary layer scheme and five-layer thermal diffusion land surface scheme. The Kain-Fritsch cumulus scheme was not used for d03 domain. The simulation starts at 12:00 UTC on 22 June and ends at 12:00 UTC on 23 June 2016."

L 416: See earlier comment concerning "rich" and "widely distributed". Also, I would suggest that when discussing results that involve vertical profiles of data, don't use the terms "high" and "low" to describe data values. Instead, use "large" and "small".

Response: We are sorry for the poor writing. Thanks so much for helping us with the English. These terms and sentences have been corrected.

L 421: See my earlier comment about the missing Yin et al. (2017) reference.

Response: Thanks for pointing out. The reference of Yin et al. (2017) has been added, as can be seen in "response to comment L372".

L 425-428: Does this mean that the assumed rime mass fraction, and therefore the adjustment factor "f" was uniform with height for each simulated profile (since liquid water path is a column variable)? Also, are you saying that you treated the rime mass fraction as liquid water for the purpose of refractive index calculations?

Response: The adjustment factor "f" increased as the height decreased. Sorry for the inaccurate statement. The sentence has been rewritten. "According to Mason et al (2018) and Moisseev et al (2017), we assumed that the rime mass fraction increased linearly with liquid water path. The ELWP was defined as the vertical integration of liquid water content (LWC), i.e., $ELWP = \int_h^\infty LWCdz$, where h is the height."

For the refractive index, it was calculated according to the volume fraction of water (f_w). With the rime mass fraction, the density-diameter relation can be obtained, and then the f_w can be obtained according to the relationship between density and f_w in Eq. (16).

L 429: But you adjusted the PSD so that the water contents in the simulated profile matched the water contents output by the model, yes?

Response: Yes, we adjusted the PSD so that the water contents in the simulated profile matched the water contents output by the model. The sentence about the number concentration of convective cloud precipitation has been removed.

L 451-452: See my earlier comment about computing relative error with reflectivities.

Response: Thanks very much for the comment. The calculation of relative error has been checked.

L 463: You mean the sensitivity of reflectivity to D_0? When describing sensitivities, try to express them as "the sensitivity of x to changes in y" so that the meaning is clear.

Response: Thanks very much for your valuable suggestion. Yes, we mean the sensitivity of reflectivity to D_0. The sentence has been rewritten. "The sensitivity of radar reflectivity to changes in D_0 in the Gamma distribution was approximately 5–10-fold greater than that of μ; the variation in μ can cause reflectivity changes of less than 10 %."

L 463-467: You mean the sensitivity of reflectivity to D_0? When describing sensitivities, try to express them as "the sensitivity of x to changes in Y" so that the meaning is clear. Yes, by imposing the empirical constraints on the PSD, the PSD itself has few degrees of freedom compared to a PSD with independent variations in parameters, so the PSD is less variable. Is this an unexpected result? Finally see my earlier comment about computing relative changes in reflectivity - be sure these percentages are calculated correctly.

Response: Thanks very much for your suggestion. Yes, by imposing the empirical constraints on the PSD, the PSD itself has few degrees of freedom compared to a PSD with independent variations in parameters, so the PSD is less variable. This is not an unexpected result. This gives the quantitative value of the reduction of reflectivity uncertainty through sensitivity analysis and demonstrates the importance of the constraint on PSD modeling.

Thanks for reminding. The calculation of relative changes in reflectivity has been checked.

L 467-468: How does the particle density affect the PSD? In general the particle density (as defined by the coefficient "a" and exponent "b" of the mass power law) are considered independent of the PSD paramemters.

Response: Sorry for the unclear description. The sentence has been rewritten. "The mass-diameter relationships for snow and graupel differ substantially for different particle habit types, which not only affects the particle scattering properties, but also affects the shape of PSD. Using the exponential PSD with a power-law mass spectrum for snow and graupel, we found that the effects of prefactor *a* on radar reflectivity were significantly. Variation in *a* mainly via changes in the particle scattering properties may result in reflectivity uncertainty of approximately 45 % for snow and 30 % for graupel."

L 469-472: But is this sensitivity due to the increase in "a" changing the scattering properties of particles, or is it because the increase in "a" increases the water content for the population of the particles? These two effects need to be separated, otherwise the influence of the change in "a" is overestimated. Also, see my earlier comment about computing fractional sensitivities for reflectivity.

Response: The water content (W) remains constant when analyzing the sensitivity of reflectivity to particle density parameters (prefactor "a" and exponent "b"). "Variation in *a* mainly via changes in the particle scattering properties may result in reflectivity uncertainty of approximately 45 % for snow and 30 % for graupel."

The calculation of fractional sensitivities for reflectivity has been checked.

L 480-481: Relative errors in what? Also, see my earlier comment about computing fractional errors in reflectivity.

Response: These are relative errors in radar reflectivity profile between the simulation and CloudSat data ($|Z_s - Z_c| / Z_c$, where Z_s is simulated reflectivity and Z_c is CloudSat observed reflectivity in mm^6/m^3). "The average relative errors in radar reflectivity profile between the simulation and

CloudSat data were within 20 %, which improved by 20–80 % compared with the conventional setting.” The calculation of fractional errors in reflectivity has been checked.

L 724: It’s not clear what is meant by "before", "during", and "after" attenuation. I’m guessing that panel (f) shows the unattenuated reflectivities, panel (g) shows the attenuation (is this one-way or two-way?), and panel (h) shows attenuated reflectivities. Is that correct?
Response: Yes, you are right. Thanks for your comment. The terms have been corrected. “(f) Simulated unattenuated radar reflectivity with the total hydrometeors, (g) two-way attenuation, and (h) attenuated radar reflectivity.”

For further improving the fluency of reading the manuscript, we have paid another commercial editing service to polish our manuscript for the language. We would like to thank the reviewer for his/her significant effort to suggest changes for our manuscript.

Special thanks to the reviewer for the valuable comment and his/her patience.
